

Feasibility study of multi-purpose quality assurance phantom for pretreatment verification of volumetric modulated arc therapy

H.S. Won^{1, 2}, J.B. Chung^{1*}, K.Y. Eom¹, D.G. Hwang^{2*}, S.W. Kang³,
T. S. Suh³

¹Department of Radiation Oncology, Seoul National University Bundang Hospital, Seongnam, Korea

²Department of Biomedical Engineering, Sangji University, Wonju, Korea

³Department of Biomedical Engineering and Research Institute of Biomedical Engineering, College of Medicine, The Catholic University of Korea, Korea

ABSTRACT

Background: The purpose of this study was to evaluate the feasibility of a multi-purpose quality assurance (QA) phantom for pretreatment verification of volumetric modulated arc therapy (VMAT). **Materials and Methods:** The QA phantom was constructed with polymethyl methacrylate (PMMA) to perform relative dosimetry using EBT3 film and MapCHECK, as well as absolute dosimetry using an ionization chamber. The QA phantom was constructed to perform relative dosimetry using EBT3 film and MapCHECK, as well as the absolute dosimetry using ionization chamber. In order to verify the pretreatment plans, 25 patients treated with VMAT were selected. The pretreatment plans were calculated in the Eclipse treatment planning system using the Acuros XB dose calculation algorithm and CT images for the QA phantom, with the same beam setup and monitor units (MUs) as those for patient treatment. All plans were delivered to the Varian TrueBeam accelerator equipped with a high-definition multi-leaf collimator. **Results:** The multi-purpose QA phantom is developed for convenient VMAT dose verification. By using the QA phantom, all 25 cases passed $\pm 3\%$ acceptability criteria in absolute dosimetry with an ionization chamber for pretreatment verification. The relative dosimetry using EBT3 film and MapCHECK system also showed high agreement of more than 90% for 2%/2-mm and 3%/3-mm criteria. **Conclusion:** The results of this study demonstrated the good multi-purpose capabilities of the phantom for the absolute and relative dosimetry. Therefore, the developed multi-purpose QA phantom was applied in our institution for routine VMAT dose verification.

Keywords: Volumetric modulated arc therapy, phantom, absolute dosimetry, relative dosimetry.

► Original article

*Corresponding authors:

Dr. J.B. Chung, D.G. Hwang,

Fax: +82 31 787 4019

+82 33 738 9962

E-mail:

jbchung1213@gmail.com

dghwang@samgji.ac.kr

Revised: July 2017

Accepted: August 2017

Int. J. Radiat. Res., July 2018;
16(3): 279-287

DOI: 10.18869/acadpub.ijrr.16.3.279

INTRODUCTION

Intensity-modulated radiation therapy (IMRT) and volumetric arc therapy (VMAT) are highly conformal external beam techniques characterized by steep in-field dose gradients, which allows better conformality of dose to the planning target volume (PTV) and better avoidance of organs at risk (OARs). These

delivery techniques have the potential to deliver optimal dose distributions when compared to conventional three-dimensional radiation therapy, and they have recently become widely used in various treatment sites, including head and neck, lung, prostate, and rectum ^(1, 2).

Pretreatment quality assurance (QA) measurements for complex techniques such as IMRT, intensity modulated arc therapy (IMAT),

and VMAT are important to ensure accurate radiation delivery, and many QA devices and techniques have been used for verifying pretreatment plans ⁽³⁻⁵⁾. Pretreatment QA is usually performed to validate the dose calculation with the treatment planning system (TPS). Before patient treatment with the plan generated on TPS, dosimetric QA procedures can be performed with the absolute and relative dosimetry for verifying treatment plan. American Association of Physicist in Medicine (AAPM) Task Group 120 reported many methods for pretreatment verification with a point dose and two-dimensional (2D) dosimetry ⁽⁶⁾.

A typical method for absolute dosimetry is the evaluation of the dose discrepancy between the calculated and measured dose at a reference point with various dosimeters such as the ionization chamber, diode detector, and thermoluminescent dosimeter. Although the measurement of absolute point dose using an ionization chamber should be performed while carefully considering chamber characteristics such as the volume averaging effect, energy response dependence, and stem cable effect, the use of an ionization chamber has the advantages of linear response to absorbed dose, small directional dependence, and excellent stability as a primary calibration standard ⁽⁷⁻¹²⁾.

Relative dosimetry measurement involves the determination of the overall agreement between the measured and computed dose distributions. The measured distributions were obtained with two-dimensional (2D) dosimeters such as radiographic films, array detectors, or electronic portal imaging devices (EPIDs). Film dosimetry, which has high spatial resolution, is generally considered a standard method for verifying the planar dose distribution with IMRT ⁽¹³⁾. Because the accuracy and precision of film dosimetry are dependent on the measurement and stringent processing conditions, film dosimetry is not a suitable method for absolute measurement. However, it is a valuable tool for relative measurements and periodic QA measurements ⁽¹⁴⁻²⁰⁾. 2D array systems are advantageous in that they can reduce the QA workload with the real-time readout and easy application, although

they have an angular dependence for the incident beam, in addition to low spatial resolution and large active area compared to film dosimetry ^(21, 22). Furthermore, 2D array systems have been proven to be more time efficient because the analysis can be performed without any further calibration or scanning procedures. Therefore, many 2D array systems have been used to perform dosimetric QA of IMRT and VMAT in previous papers ⁽²³⁻²⁶⁾.

The pretreatment verification measurement to ensure that the treatment dose was delivered within clinically acceptable tolerance was performed in many clinical centers by applying in-house or commercial phantoms using several dosimeters ⁽²⁷⁻²⁹⁾. In order to conduct pretreatment verification for the patient therapy plan, we reconstructed a multi-purpose phantom that can perform absolute and relative dosimetry by utilizing an ionization chamber, Gafchromic film, and MapCHECK array system. The purpose of this study was to evaluate the feasibility of the multi-purpose QA phantom for the pretreatment verification of VMAT.

MATERIALS AND METHODS

Construction of multi-purpose QA phantom

A multi-purpose QA phantom was constructed using polymethyl methacrylate (PMMA; $\rho = 1.19 \text{ g/cm}^3$) to utilize an ionization chamber, an EBT3 film, and a MapCHECK system. The phantom is composed of four or five slabs with horizontal and vertical dimensions of 315 and 300 mm, respectively. In the basic configuration of the phantom, it has a total height of 186 mm with four slabs having thicknesses of 30, 50, 56, and 50 mm as shown in figure 1. A hole that holds an ionization chamber (PTW CC13; PTW, Freiburg, Germany) was made at the center (43 mm height from the bottom of the 56 mm slab) of the phantom so that it can be inserted into the chambers (figure 1A). A film for the 2D relative dosimetry (Gafchromic EBT3; ISP, Ashland) was inserted in the 56 mm slab by splitting it into slabs having thicknesses of 13 mm and 43 mm (figure 1B). A MapCHECK system (MapCHECK;

SUN NUCLEAR Corporation) was designed to be inserted in the 56 mm slab (figure 1C). The measuring point of the ionization chamber, EBT3 film, and MapCHEDK system is 93 mm in the bottom direction from the top of the phantom.

Planning and delivery for verification plan

25 patients who completed treatment in our center for prostate, lung, and head and neck (H&N) cancer were selected in this study. All treatment plans were generated by employing Eclipse (Ver. 11.0.34, Varian Medical Systems) TPS with the TrueBeam STx accelerator (Varian Medical Systems, Palo Alto, CA, USA), which is a high-definition multileaf collimator (HD MLC). Depending on the plan, 6- and 10-MV flattening filter-free (FFF) beams were used. Dose computations were calculated with the Acuros XB algorithm (AXB, version 11) and a 2.5-mm dose grid. For all VMAT plans, one or two arcs were used in treatment planning. In order to estimate the absolute and relative dosimetry, the pretreatment plans were recomputed in the computed tomography images for each QA phantom, with the same beam setup and monitor units (MUs) as in the treatment plans. Table 1 lists the characteristics of pretreatment verification QA plans for all patients.

By using the constructed multi-purpose QA phantom, a point dose measurement was carried out with the ionization chamber, as shown in figure 1A. The 2D dose distribution was measured with the film and the diode array system, as shown in figure 1B and C. Before each measurement, the multi-purpose QA phantom was localized with the cone-beam CT of X-ray imaging systems. The QA phantom position was determined to be localized within 1° and 1 mm of the reference verification planning image before the verification fields were delivered.

Dosimetric comparison in multi-purpose phantom

Prior to the pretreatment verification, the daily linear accelerator output was checked with a Farmer-type ion chamber by applying the TG51 protocol on the day of the calibration, and the pretreatment was delivered after checking

routine dynamic MLC quality control using EPID to improve accuracy⁽³⁰⁾. The MLC tests include the picket fence, weeping gap, and MLC speed tests. Previously, Vieilleveigne *et al.* reported that dose distributions are more sensitive to MLC errors than to collimator, couch, or gantry errors⁽³¹⁻³³⁾.

Absolute dosimetry was measured in the multi-purpose phantom by using the ionization chamber, as shown in figure 1A. Absorbed dose was measured with response of electrometer after applying conversion factors as per international dosimetry protocol. The percentage difference (%Diff) in the calculated dose was evaluated for comparison with the measured dose at the same depth position. The %Diff was calculated using equation (1).

$$\%Diff = \frac{(Measured\ dose - Calculated\ dose)}{Calculated\ dose} \times 100 \quad (1)$$

A Gafchromic EBT3 film of dimensions 20 × 25.4 cm² for 2D dosimetry has been used in this study. Film calibration was performed in a solid water phantom, and a net-optical density (netOD) curve was obtained in a field size of 10 × 10 cm² with a 6-MV FFF beam. Doses ranging from 0 to 10 Gy were irradiated to convert the measured OD to absolute dose. All irradiated films were scanned with a flatbed scanner (Epson Expression 11000 XL, Epson America INC., Long Beach, CA) after irradiation for at least 24 hours. This calibration netOD curve was imported into the software Radiological Imaging Technology 113 (RIT 113, Ver. 6.4, Colorado Springs, Co, USA), as shown in figure 2. The EBT3 film was placed in the multi-purpose QA phantom and irradiated with the treatment fields. The measured dose distribution using the EBT3 film was compared with the calculated dose distribution for analyzing gamma agreement with RIT 113.

The MapCHECK system was used in this study as a second dosimetric detector for 2D dosimetry. The MapCHECK system consists of 445 N-type solid-state diodes that are in a 22 × 22 cm² 2D diode array. Before the measurement of 2D dose distribution, the MapCHECK system was measured the background in the treatment room and performed the array and dose

calibration. The background calibration was processed automatically for 30 seconds after it was connected to the MapCHECK system and analysis software when running the program. Array calibration is the process of setting up a proper reading of the relative proportions between each diode and the center diode. 200 MU was delivered for this procedure while rotating the MapCHECK system by 90° clockwise. The dose calibration was performed for setting the absolute dose of the detector. For dose calibration, a dose of 200 cGy was irradiated on a field size of 10 × 10 cm², source-to-axis distance of 100 cm. After the calibration, the measured dose distribution of verification plans was obtained using MapCHECK system with the phantom. The measured dose distribution was compared with the calculated dose distribution in the gamma agreement analysis using the MapCHECK software.

The coronal plan at the isocenter slice of the phantom was selected for the gamma evaluation. This was intended to represent what is most commonly performed in clinical practice when a VMAT plan is evaluated using a film and a 2D array system. The gamma index used for analyzing 2D dosimetry was applied in two scenarios, 3%/3-mm and 2%/2-mm, of dose difference and distance to agreement (DTA), respectively. Based on the gamma evaluation, the pixels (threshold value: 10) that received less than 10% of the maximum dose were not considered. The passing rate via gamma analysis was calculated with gamma points less than 1 ($\gamma < 1$), indicating that the points lie within the dose difference and DTA passing criteria. To express the box plot with the passing rates of 2D dosimetry, the data were analyzed using Statistical Package for the Social Sciences (SPSS, version 20.0, SPSS Inc., Chicago, IL) software.

Table 1. Characteristics of pretreatment verification quality assurance plans for 25 patients

Patient No.	Energy (MV)	No. of arcs	Ionization chamber		EBT3		MapCHECK	
			MU	DPR (cGy)	MU	DPR (cGy)	MU	DPR (cGy)
1	6	2	290/287	199.7	681/673	462.8	340/336	219.2
2	10	2	317/324	199.7	870/887	531.8	435/443	250.0
3	10	1	575	199.4	1664	562.1	908	292.0
4	10	2	285/282	199.4	710/703	481.5	355/352	227.8
5	6	2	326/340	199.8	700/731	425.1	350/366	199.1
6	6	2	405/414	199.5	1037/1062	497.9	519/531	232.1
7	6	2	286/298	199.7	760/791	525.2	380/395	246.1
8	6	2	334/338	199.9	799/808	469.8	399/404	217.8
9	6	2	357/368	200	726/748	402.7	363/374	189.3
10	6	2	326/369	199.6	727/824	440.6	364/412	206.4
11	10	2	260/277	199.4	749/798	562.5	340/363	243.8
12	10	2	258/271	199.8	728/763	551.8	331/347	237.3
13	10	2	280/279	200	787/782	588.0	358/355	254.5
14	10	2	229/237	199.5	682/703	582.0	310/320	253.3
15	10	2	326/332	199.7	978/997	430.2	489/499	209.6
16	10	1	515	199.8	1429	559.1	715	276.9
17	10	1	639	199.8	1610	503.4	805	251.4
18	10	1	566	199.7	1393	493.6	697	245.6
19	10	1	781	199.9	2179	562.9	1089	278.7
20	10	2	292/336	200	827/950	570.5	413/475	284.6
21	10	2	279/310	199.6	809/899	388.5	405/449	181.8
22	10	1	524	199.9	1471	564.3	735	280.0
23	10	2	241/242	199.7	708/711	588.9	354/356	292.4
24	10	1	541	199.6	1598	550.2	799	275.8
25	10	1	555	199.5	1527	552.1	694	250.4



Figure 1. A multi-purpose phantom using (A) the ionization chamber, (B) the EBT3 film, and (C) the MapCHECK system.

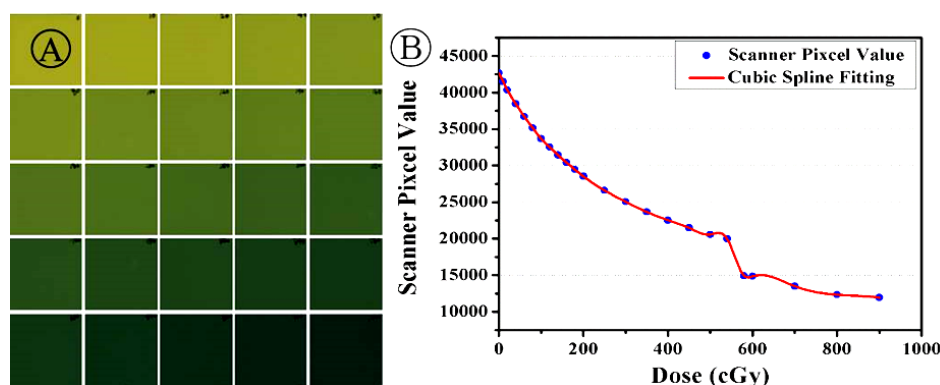


Figure 2. Net-optical density curve of the Gafchromic EBT3 film for the 6 MV flattening-filter-free beams: (A) the scan images of the irradiated EBT3 film and (B) the net-optical density curve generated by RIT 113 software.

RESULTS

In this study, we developed a multi-purpose QA phantom for conventional IMRT dose verification. Using this QA phantom, absolute and relative dosimetry for pretreatment verification was performed under the same conditions as for the patient treatment. For the 25 selected patients, the evaluation of dose discrepancy between the calculated and measured dose for the composite plan has been performed with an ionization chamber after the patients were treated with VMRT. A histogram of this data is shown in figure 3. The largest dose difference was -2.95%, with a mean of only -0.35% and standard deviation of 1.93%. According to our clinic standard acceptability criterion of $\pm 3\%$, all of 25 pretreatment plans were acceptable for VMRT treatment. The largest dose difference occurred in a treatment plan with usually large intensity modulation, whereas the measured doses at regions with lower intensity modulation were in better agreement with the calculated dose. The

negative-to-positive ratio of the dose difference is 0.92, and the mean dose difference is a negative value.

Figure 4A and B show examples of the gamma evaluation result for dose distributions measured using the EBT3 film and MapCHECK system in comparison with the TPS-generated dose distribution. The statistical summary of passing rate via gamma analysis for the EBT3 film and MapCHECK system is shown in figure 5 for both 2%/2-mm and 3%/3-mm criteria. For EBT3 film, the passing rate ranged from 91.9% to 99.5% for 2%/2-mm and 97.1% to 99.9% 3%/3-mm, respectively. The average and standard deviation of the passing rate were $97.1\% \pm 2.1\%$ for 2%/2-mm and $99.4\% \pm 0.8\%$ for 3%/3-mm. The median gamma passing rate was 97.9% and 99.7% for 2%/2-mm and 3%/3-mm, respectively. For MapCHECK system, the passing rate ranged from 97.7% to 100% for 3%/3-mm and 91.7% to 98.7% for 2%/2-mm. The average and standard deviation of passing rate were $99.0\% \pm 0.8\%$ for 3%/3-mm and $95.6\% \pm 1.5\%$ for 2%/2-mm, respectively. The median gamma

passing rate was observed to be 95.8% for 2%/2-mm and 98.9% for 3%/3-mm, respectively.

The EBT3 film and MapCHECK system for 2D dosimetry showed high levels of agreement greater than 90% for both criteria. In particular, the gamma agreement for the 3%/3-mm criterion was greater than 97% in all the cases. Better agreement was observed with the EBT3 film than with the MapCHECK system. However, the EBT3 film dosimetry needed careful evaluation of scanner and film performance, which has been mainly attributed to

non-uniform film response. The minimum passing rate was observed in the MapCHECK system for stricter 2%/2-mm criteria, which might be due to the large dose gradient in the delivered dose and the limited resolution of the the MapCHECK system to detect the dose distribution for the small sized target. However, the overall results of 2D dosimetry obtained using the multi-purpose phantom applying the EBT3 film and MapCHECK system were satisfactory with good agreement between the calculated and measured dose distributions.

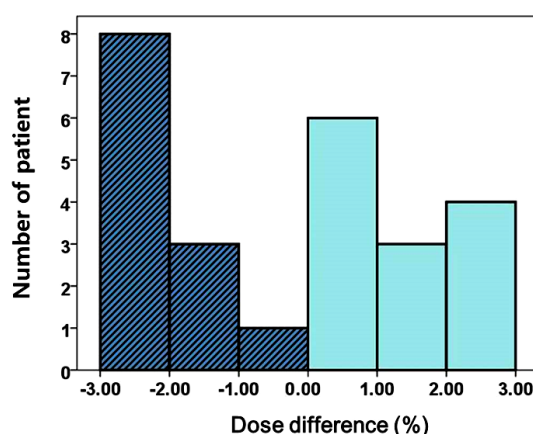


Figure 3. A histogram of the measured and calculated absolute dose differences for 25 patients.

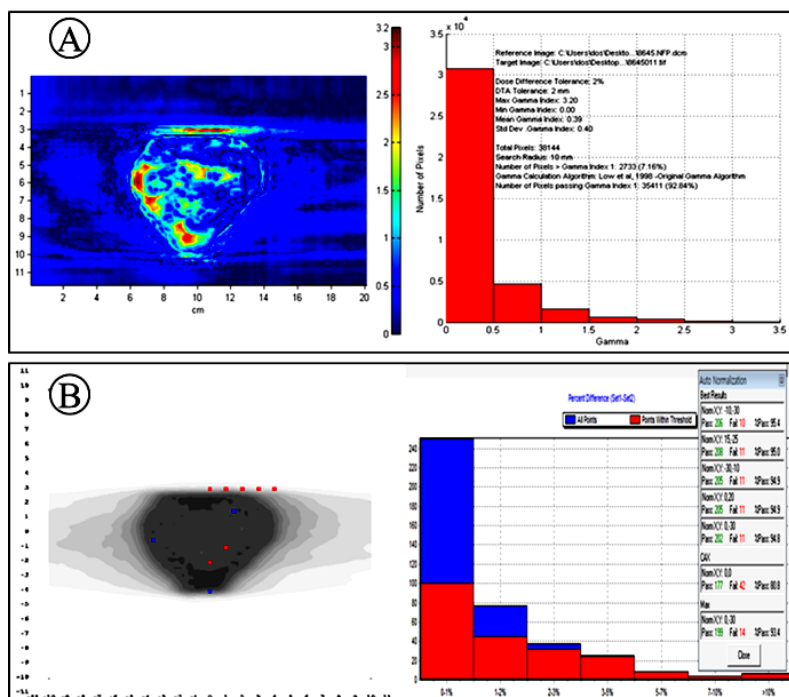


Figure 4. The gamma evaluation result for dose distributions measured using (A) the EBT3 film and (B) MapCHECK in comparison with the TPS-generated dose distribution.

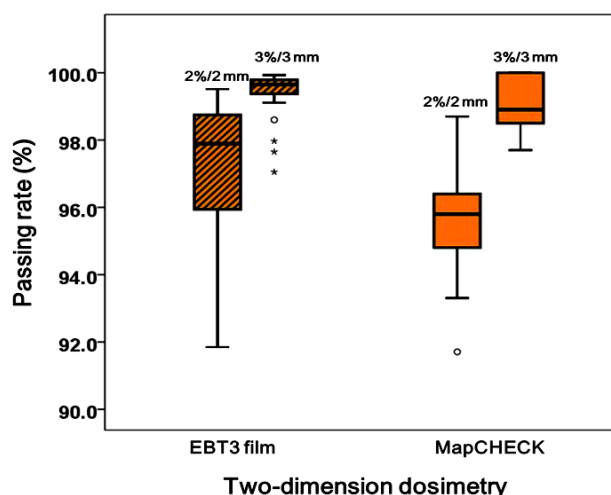


Figure 5. The statistical passing rate for the EBT3 film and MapCHECK system by gamma analysis.

DISCUSSION

Accurate verification of pretreatment for VMAT or IMRT technique is increasingly taking on added importance (33,34). For this reason, the use of IMRT QA based on phantoms has gradually increased. Commercial QA phantoms are commonly used, but some phantoms are also used by in-house customization. In this study, the developed QA phantom is advantageous in that it can be applied multi-purpose for both absolute and relative dosimetry. The QA phantom was used to measure absolute point dose measurement using ionization chamber as well as to verify planar dose distribution using EBT3 film and MapCHECK system in the phantom (figure 1). The QA phantom was more convenient for routine clinical use with the reproducible and exact setup compared to the water phantom. In addition, the QA phantom that adopts multicross checks with different dosimeters can provide more accurate dosimetry evaluation. For absolute dosimetry using the QA phantom, our results are comparable with the findings at other institutions (35,36). The differences between the calculated and measured dose using a QA phantom were always found within $\pm 3\%$, and in half of cases these showed within $\pm 2\%$, while the other half were above $\pm 2\%$. Also, gamma passing rates showed a good agreement of more than 90% for both the criteria of 2%/ 2-mm and

3%/ 3-mm. Based on the results for absolute and relative dosimetry, this study demonstrated that the multi-purpose QA phantom has sufficient potential for pretreatment verification of VMAT technique.

The current QA phantom has two limitations; the rectangular shape and homogeneous phantom. Generally, the patients-specific dosimetry for VMAT or IMRT demands ideal phantom geometry such as cylindrical or thoracic shape. The sharp edge of our rectangular phantom could be caused perturbation in the dosimetric results by the oblique irradiation field and the error of geometry setup. Park et al also reported that the dosimetric results with cylindrical phantom obtained better outcomes for 2D dosimetry (33). However, in Kinhikar *et al.* study on the patient-specific QA of VMAT, no statistically significant differences were founded for point dose measurement with an ionization chamber between cylindrical and rectangular phantoms (34). In order to simulate the real dose delivered to the patient, the heterogeneous phantom that was considered similar to human body was recommended to be used (37,38). However, most of available dosimetric phantoms have almost homogeneous density (33-35). The QA phantom used in this study was made with PMMA material having homogeneous density. Therefore, our QA data were checked the dose computed for the homogeneous QA phantom,

not the dose for the heterogeneous anatomy of a patient. In the future study, investigation of pretreatment verification for VMAT technique on heterogeneous artificial phantom with cylindrical geometry and thoracic shape should be established to achieve the accurate outcome for the patient-specific QA.

CONCLUSION

In this study, a multi-purpose phantom was developed to perform pretreatment verification for VMAT technique. We compared the calculated dose and dose distribution using TPS with the measured data using the phantom. The QA results show that the multi-purpose phantom has good capabilities for absolute and relative dosimetry. Thus, the constructed multi-purpose phantom has been applied for routine VMRT dose verification at our institution since 2015.

ACKNOWLEDGMENTS

This work was supported by Grant No. 14-2015-016 from the Seoul National University Bundang Hospital (SNUBH) Research Fund and a grant of the Korea Health Technology R&D Project through the Korea Health Industry Development Institute (KHIDI), funded by the Ministry of Health and Welfare, Republic of Korea (Grant Number: HI15C0638).

Conflicts of interest: Declared none.

REFERENCES

1. Chung JB, Kang SW, Eom KY, Song C, Choi KS, Suh TS (2016) Comparison of Dosimetric Performance among Commercial Quality Assurance Systems for Verifying Pretreatment Plans of Stereotactic Body Radiotherapy Using Flattening-Filter-Free Beams. *J Korean Med Sci*, **31**: 1742-1748.
2. Mattes MD, Zhou Y, Berry SL, Barker CA (2016) Dosimetric comparison of axilla and groin radiotherapy techniques for high-risk and locally advanced skin cancer. *Radiat Oncol J*, **34**: 145-155.
3. Carrasco P, Jornet N, Latorre A, Eudaldo T, Ruiz A, Ribas M (2012) 3D DVH-based metric analysis versus per-beam planar analysis in IMRT pretreatment verification. *Med Phys*, **39**: 5040-5049.
4. Pecharromás-Gallego R, Mans A, Sonke JJ, Stroom JC, Olaciregui-Ruiz I, van Herk M, Mijnheer BJ (2011) Simplifying EPID dosimetry for IMRT treatment verification. *Med Phys*, **38**: 983-992.
5. Grigorov G, Chow JCL, Yazdani N (2010) Dosimetry limitations and pre-treatment dose profile correction for sliding window IMRT. *Int J Radiat Res*, **8**: 61-74.
6. Low DA, Moran JM, Dempsey JF, Dong L, Oldham MI (2011) Dosimetry tools and techniques for IMRT. *Med Phys*, **38**: 1313-1338.
7. Low DA, Dempsey JF, Wahab S, Huq S (2003) Ionization chamber volume averaging effects in dynamic intensity modulated radiation therapy beams. *Med Phys*, **30**: 1706-1711.
8. Agostinelli S, Garelli S, Piergentili M, Foppiano F (2008) Response to high-energy photons of PTW31014 PinPoint ion chamber with a central aluminum electrode. *Med Phys*, **35**: 3293-3301.
9. Wulff J, Heverhagen JT, Zink K (2008) Monte-Carlo-based perturbation and beam quality correction factors for thimble ionization chambers in high-energy photon beams. *Phys Med Biol*, **53**: 2823-2836.
10. McEwen MR (2010) Measurement of ionization chamber absorbed dose kQ factors in megavoltage photon beams. *Med Phys*, **37**: 2179-2193.
11. Martens C, De Carlos C, De Neve W (2000) The value of the PinPoint ion chamber for characterization of small field segments used in intensity-modulated radiotherapy. *Phys Med Biol*, **45**: 2519-2530.
12. Dong L, Antolak J, Salehpour M, Forster K, O'Neill L, Kendall R, Rosen I (2003) Patient-specific point dose measurement for IMRT monitor unit verification. *Int J Radiat Oncol Biol Phys*, **56**: 867-877.
13. Pallotta S, Marrazzo L, Bucciolini M (2007) Design and implementation of a water phantom for IMRT, arc therapy, and tomotherapy dose distribution measurements. *Med Phys*, **34**: 3724-3731.
14. Mizuno H, Takahashi Y, Tanaka A, Hirayama T, Yamaguchi T, Katou H, Takahara K, Okamoto Y, Teshima T (2012). Homogeneity of GAFCHROMIC EBT2 film among different lot numbers. *J Appl Clin Med Phys*, **13**: 198-205.
15. Park S, Kang SK, Cheong KH, Hwang T, Kim H, Han T, Lee MY, Kim K, Bae H, Su Kim H, Han Kim J, Jae Oh S, Suh JS (2012) Variations in dose distribution and optical properties of GafchromicTM EBT2 film according to scanning mode. *Med Phys*, **39**: 2524-2535.
16. Méndez I, Peterlin P, Hudej R, Strojnik A, Casar B (2014) On multichannel film dosimetry with channel-independent perturbations. *Med Phys*, **41**: 011705.
17. Lewis DF, Chan MF (2016) Technical Note: On GAFChromic EBT-XD film and the lateral response artifact. *Med Phys*, **43**: 643-649.
18. Lewis D, Micke A, Yu X, Chan MF (2012) An efficient protocol for radiochromic film dosimetry combining calibration

- and measurement in a single scan. *Med Phys*, **39**: 6339-6350.
19. Devic S, Aldelaijan S, Mohammed H, Tomic N, Liang HK, DeBlois F (2010) Absorption spectra time evolution of EBT-2 model GAFCHROMIC™ film. *Med Phys*, **37**: 2207-2214.
20. Butson MJ, Cheung T, Yu PK (2009). Evaluation of the magnitude of EBT Gafchromic film polarization effects. *Australas Phys Eng Sci Med*, **32**: 21-5.
21. Wiezorek T, Banz N, Schwedas M, Scheithauer M, Salz H, Georg D, Wendt TG (2005) Dosimetric Quality Assurance for Intensity-Modulated Radiotherapy. *Strahlenther Onkol*, **181**: 468-474.
22. Létourneau D, Gulam M, Yan D, Oldham M, Wong JW (2004) Evaluation of a 2D diode array for IMRT quality assurance. *Radiother Oncol*, **70**: 199-206.
23. Kim YL, Chung JB, Kim JS, Lee JW, Choi KS (2014) Comparison of the performance between portal dosimetry and a commercial two-dimensional array system on pretreatment quality assurance for volumetric-modulated arc and intensity-modulated radiation therapy. *J Korean Phys Soc*, **64**: 1207-1212.
24. Park JH, Lee HR, Kim CH, Kim SH, Kim S, Lee SB (2015) Development of Two-dimensional Prompt-gamma Measurement System for Verification of Proton Dose Distribution. *Prog Med Phys*, **26**: 42-51.
25. Son J, Baek T, Lee B, Shin D, Park SY, Park J, Lim YK, Lee SB, Kim J, Yoon M (2015) A comparison of the quality assurance of four dosimetric tools for intensity modulated radiation therapy. *Radiol Oncol*, **49**: 307-313.
26. Swamy S, Radha C, Arun G, Kathirvel M, Subramanian V (2016) Performance evaluation of gated volumetric modulated arc therapy. *Int J Radiat Res*, **14**: 81-90.
27. Burman C, Chui CS, Kutcher G, Leibel S, Zelefsky M, LoSasso T, Spirou S, Wu Q, Yang J, Stein J, Mohan R, Fuks Z, Ling CC (1997) Planning, delivery, and quality assurance of intensity modulated radiotherapy using dynamic multileaf collimator: Strategy for large-scale implementation for the treatment of carcinoma of the prostate. *Int J Radiat Oncol Biol Phys*, **39**: 863-873.
28. Miles EA, Clark CH, Urbano MT, Bidmead M, Dearnaley DP, Harrington KJ, A'Hern R, Nutting CM (2005) The impact of introducing intensity modulated radiotherapy into routine clinical practice. *Radiother Oncol*, **77**: 241-246.
29. Ezzell GA, Burmeister JW, Dogan N, LoSass TJ, Mechalakos JG, Mihailidis D, Molineu A, Palta JR, Ramsey CR, Salter BJ, Shi J, Xia P, Yue NJ, Xiao Y (2009) IMRT commissioning: multiple institution planning and dosimetry comparisons, a report from AAPM Task Group 119. *Med Phys*, **36**: 5359-5373.
30. Almond PR, Biggs PJ, Coursey BM, Hanson WF, Saiful M, Nath R, Rogers DW (1999) AAPM Task Group No. 51, Protocol for Clinical Reference Dosimetry of High-Energy Photon and Electron Beams. *Med Phys*, **26**: 1847-1870.
31. Chang KH, Ji Y, Kwak J, Kim SW, Jeong C, Cho B, Park J, Yoon SM, Ahn SD, Lee S (2016) Clinical implications of high definition multileaf collimator dosimetric leaf gap variations. *Prog Med Phys*, **27**: 111-116.
32. Lee SS, Choi SH, Min CK, Kim WC, Ji YH, Park S, Jung H, Kim MS, Yoo HJ, Kim KB (2015) Assessment for the utility of treatment plan QA system according to dosimetric leaf gap in multileaf collimator. *Prog Med Phys*, **26**: 168-177.
33. Park JY, Lee JW, Choi KS, Lee JS, Kim YH, Hong S, Suh TS (2011) Development of a novel quality assurance system based on rolled-up and rolled-out radiochromic films in volumetric modulated arc therapy. *Med Phys*, **38**: 6688-6696.
34. Kinikar RA, Pandey VP, Jose RK, Mahantshetty U, Dhote DS, Deshpande DD, Shrivastava SK (2013) Investigation on the effect of sharp phantom edges on point dose measurement during patient-specific dosimetry with Rapid Arc. *J Med Phys*, **38**: 139-142.
35. Ma CM, Jiang SB, Pawlicki T, Chen Y, Li JS, Deng J, Boyer AL (2003) A quality assurance phantom for IMRT dose verification. *Phys Med Biol*, **48**: 561-572.
36. Price RA, McNeeley S, Ma C, Chen L, Li JS, Ding M, Fourkal E, Qin L (2002) A practical method for dose determination using a non-water phantom for IMRT quality assurance. *Med Phys*, **29**: 1267(abstract).
37. Senthilkumar S (2014) Design of homogeneous and heterogeneous human equivalent thorax phantom for tissue inhomogeneity dose correction using TLD and TPS measurements. *Int J Radiat Res*, **12**: 169-178.
38. Gurjar OP, Mishra SP, Bhandari V, Pathak P, Patel P, Shrivastav G (2014) Radiation dose verification using real tissue phantom in modern radiotherapy techniques. *J Med Phys*, **39**: 44-49.

